JOURNAL OF Materials CHEMISTRY

A computer simulation study of vanadium substitution in the $AlPO_4$-5 framework

Jorge Gulín-González,*[a] José de la Cruz Alcaz,[a] J. M. López Nieto[b] and Carlos de las Pozas[c]

[a]*Instituto Superior Politécnico José A. Echevarría (ISPJAE), Dpto. de Física, Marianao, La Habana, Cuba. E-mail: gulin@quimica.cneuro.edu.cu*
[b]*Instituto de Tecnología Química, UPV-CSIC, Univ. Politécnica de Valencia, Avda. Los Naranjos s/n, Valencia, Spain 46071*
[c]*National Center for Scientific Research, Division of Chemistry, P.Box 6990, La Habana, Cuba*

Received 16th March 2000, Accepted 18th July 2000
First published as an Advance Article on the web 6th October 2000

The substitution of Al^{3+} by V^{3+} and P^{5+} by V^{5+} in $AlPO_4$-5 microporous materials is studied by energy minimisation techniques. The incorporation of V^{3+} in aluminium sites is accompanied by a strong distortion of the framework. The least stable site has the lower V^{3+}–O distance, and more deformed V^{3+}–O–P angles. In contrast, for the substitution of P^{5+} by V^{5+} small deformations of the framework were obtained. For this reason we suggest the vanadium is found, fundamentally, as V^{5+} in the phosphorus sites. Very similar energies were obtained for the six different independent phosphorus sites of the asymmetric unit cell which suggests that the V^{5+} ion could occupy any of these sites with the same probability. Furthermore, the 78 configurations of two V^{5+} ions in the unit cell were studied. We did not find a relationship between the stability of the framework and the position of the substituted vanadium ions. An increment of around 1% in the volume of the unit cell with respect to the configurations of one V^{5+} ion was observed. Simulation of the VAPO-5 vibrational spectrum shows a new band ($\approx 835\ cm^{-1}$), in agreement with the IR experiments.

1. Introduction

Metal substituted aluminophosphate microporous materials (MeAPOs) have been the subject of a variety of studies since their synthesis was first reported by Flanigen *et al.*[1] The introduction of transition metal ions is aimed at obtaining catalysts containing acidic as well as redox sites. This work has been reviewed by Bellussi and Rigutto.[2] VAPO-5 molecular sieves catalyse the ammoxidation of alkanes, epoxidation of alkenes, and oxidation of aromatic compounds.[3–6] VAPO-5 is also a very selective catalyst for the oxidative dehydrogenation (ODH) of propane to propene.[7,8] Isolated tetrahedral V^{5+} species in the neutral framework have been proposed as being responsible for the catalytic behaviour observed.[8,9]

The isomorphous substitution of vanadium ions in crystalline aluminophosphates has been debated by several authors.[3–5, 10–13] According to Montes *et al.*[4] and Jhung *et al.*[5] the isomorphous substitution of P^{5+} by V^{4+} and V^{5+} occurs. Rigutto and van Bekkum[3] suggested the replacement of Al^{3+} by V^{4+}. Weckhuysen *et al.*[10] have investigated the coordination of vanadium using diffuse reflectance (DRS) and electron spin resonance (ESR) spectroscopy but they did not find unambiguous evidence for isomorphous substituted vanadium in $AlPO_4$-5. Starting from IR spectroscopy and TPDA studies Martin *et al.*[11] concluded that V^{4+} does not replace P^{5+}. Bedioui *et al.*[12] found two redox processes corresponding to V(+5)/V(+4) for two distinct vanadium sites using cyclic voltammetry. On the basis of ESR and electron spin echo modulation spectroscopy studies (ESEM) Prakash and Kevan[13] concluded that as-synthesised VAPO-5 contains two VO^{2+} species with distorted octahedral symmetry. These authors have reported that during calcination a proportion of the V^{4+} ions are oxidised to V^{5+} and incorporation of vanadium into the framework phosphorus site as a localised defect is supported by ^{31}P, ^{27}Al and 2D ESEM results.

On the other hand, the structure of $AlPO_4$-5 has been extensively studied by experimental and theoretical methods.[14–22] The existence of linear Al–O–P angles found in the hexagonal structures in the earlier work gave reason for subsequent studies focused on whether they are average angles as a consequence of disorder of the oxygen around the Al–P axis or the actual angles presented in this material. Recently the structure was refined in an orthorhombic (*Pcc*2) space group with no linear Al–O–P angles,[23] and moreover computer simulation studies have found that the structure can be described in a hexagonal (*P*6) group also having no linear angles.[22,24]

In this work lattice energy minimisation techniques employing empirical interatomic potentials were used to study the incorporation of vanadium in the $AlPO_4$-5 framework (P^{5+} by V^{5+} and Al^{3+} by V^{3+}). The lattice energies of all the different structures which contain one V^{3+} ion or one V^{5+} ion in the hexagonal *P6cc* unit cell of Bennett *et al.*[14] and orthorhombic *Pcc*2 unit cell of Mora *et al.*[23] were calculated. Moreover, with the objective of studying the influence of the amount of vanadium incorporated into the framework and the interactions between these defects, different configurations of two V^{5+} ions in the unit cell were studied.

2. Methodology

The perfect lattice calculations were performed using the program GULP.[25] This program uses interatomic potentials that combine long-range electrostatic with short-range pair interactions (Buckingham potentials). We calculated electrostatic interactions by the Ewald method.[26] For the short-range interaction a cut off radius of 12 Å was employed. Polarisability of the oxygen atoms is treated using the shell model developed by Dick and Overhauser.[27] This model includes the

coupling between the short-range repulsive forces and ionic polarisation, preventing excessive polarisation of the ion. To simulate the partial covalency of the framework relaxation a three body term is included. Atomic coordinates and cell parameters were optimised to zero force using Broyden–Fletcher–Goldfarb–Shanno (BFGS)[28] and rational functional optimisation (RFO)[29] minimisation methods.

We used the Mott–Littleton methodology[30] to handle the incorporation of defects in the framework. This method explicitly relaxes an inner region (region I) with around 500 atoms surrounding the defect to minimum energy. The more distant region (region II) of the crystal is considered as a dielectric continuum. The defect energy calculations were performed with a region I radius of 8 Å and a region II radius of 20 Å. The phonon spectra were calculated at the Γ point.

All potential parameters used in the simulation are given in Table 1. The potential parameters of Gale and Henson[31] were used for modeling the interactions of P^{5+}–O^{2-} and Al^{3+}–O^{2-}. These parameters were obtained by empirical fitting of the crystal structure, elastic and dielectric properties of Berlinite. Several calculations[21–24] demonstrated the transferability of these potentials to other aluminophosphates. For V^{n+}–O^{2-} ($n=3, 5$) interactions the parameters calculated by Sayle *et al.*[32] were used. These parameters were calculated by the empirical electron gas potential method. This method provides a consistent set of potential parameters for the dopant-ion interactions. Sayle's parameters have been applied to modeling other metal–alminophosphate structures.[33]

3. Results and discussion

3.1 Substitution of one vanadium ion in aluminium or phosphorus sites in the $AlPO_4$-5 unit cell

The optimisation of the VAPO-5 unit cell was initially carried out utilising the hexagonal *P6cc* unit cell of Bennett.[14] The cell parameters obtained in the simulation and the experimental values[34] are shown in Table 2. We considered two cases: (i) the vanadium substitutes for the Al^{3+} as V^{3+} (VAPO† case) and (ii) the vanadium substitutes for the P^{5+} as V^{5+} (VAPO†† case). A good agreement between both experimental and simulated cell parameters was obtained. This agreement is more marked in the VAPO†† case. The differences could be due to the fact that the experimental data available[34] concern the uncalcined VAPO-5 (triethylamine as template) while the simulation is carried out starting from the calcined structure. This reasonable result is another point in favour of the application of the potentials reported by Sayle *et al.*[32] to metal–aluminophosphates microporous materials (MeAPOs).

Table 1 Potential parameters used in the GULP[25] code

Potential parameters Buckingham Potentials[31]			
Species	A/eV	ρ/Å	C/eV Å^{-6}
Al^{3+}–O^{2-}	1283.90	0.32052	10.66
P^{5+}–O^{2-}	877.34	0.35940	0.00
O^{2-}–O^{2-}	22764.00	0.14900	27.88
V^{3+}–O^{2-}	700.14	0.3973	6.94
V^{5+}–O^{2-}	828.54	0.3836	−1.41

Three Body Terms		
Species	k/eV rad^{-1}	θ_0/°
O–T(Al,V^{3+})–O	2.09724	109.47

Shell Model Parameters	
Species	k/eV Å^{-2}
O^{2-}	74.92

Charges					
P^{5+}	Al^{3+}	V^{5+}	V^{3+}	O^{2-} (core)	O^{2-} shell)
+5.0	+3.0	+5.0	+3.0	+0.86902	−2.86902

[a] $V=\sum_{ij}$ (Buckingham) $+\sum_{ij}$(Coulombic) $+\sum_{ijk}$(Three Body) $+\sum_{ij}$ (Core–Shell). [b] V_{ij}(Buckingham) $=A_{ij}\exp(-r_{ij}/\rho)-C_{ij}/r^6$. [c] V_{ij}(Coulombic) $=q_iq_j/r_{ij}$. [d] V_{ijk}(Three body) $=0.5k_{ijk}(\theta_{ijk}+\theta^0{}_{ijk})^2$. V_i(Core–Shell) $=0.5k_i\Delta r_i^2$ where Δr_i is the core–shell separation.

Subsequently, we performed the optimisation starting from the orthorhombic *Pcc*2 unit cell.[23] Fig. 1a shows the asymmetric unit cell of Mora *et al.*[23] with aluminium and phosphorus sites. The hexagonal *P6cc* unit cell has only one crystallographically distinct site for the phosphorus and aluminium. In contrast, the orthorhombic *Pcc*2 unit cell has six independent sites for these elements in an asymmetric unit cell. The final energy and cell parameters of the structures where one V^{3+} ion is substituted for an aluminium in each unit cell ($Al^{3+}/V^{3+}=23/1$ ratio) are shown in Table 3. In this case an energy difference between the six aluminium sites is observed (the difference between the maximum and minimum energy is $\Delta E=0.0064$ eV per tetrahedral site of Al or 0.15 eV per unit cell), with the following order of stability: T,Al(5) > T,Al(1) = T,Al(2) > T,Al(6) > T,Al(4) > T,Al(3). The substitution of Al^{3+} by V^{3+} is accompanied, as we will see, by a strong distortion in the framework, which may be unfavourable from a geometric point of view. In this case, the large V^{3+} ion (0.63 Å) may not be expected to be stable in the lattice since the radius is at the limit for isomorphic substitution based on a simplified version of Pauling's minimum radius ratio.[35]

In Table 4 we see the energies and cell parameters for the structures where a V^{5+} ion is substituted at one phosphorus site per unit cell ($P^{5+}/V^{5+}=23/1$). The six phosphorus sites have the same energy (the difference between the maximum and minimum energy is $\Delta E=0.0005$ eV per tetrahedral site or 0.012 eV per orthorhombic unit cell). These small energy differences, lower than kT at the synthesis temperature ($\approx$0.05 eV), do not allow us to distinguish one tetrahedral site from another. According to this result, the substitution of P^{5+} by V^{5+} would occur in any of the six sites for phosphorus in the unit cell with the same probability. Furthermore, the six configurations result in similar unit cell parameters (all structures possess an orthorhombic unit cell). This result is another argument in support of the hypothesis for the incorporation of the V^{5+} ion in the different tetrahedral phosphorus sites.

A corroboration of the above results was sought by performing further defect calculations. The defect energy of an isolated V^{n+} ion substituting into the framework at the most and least stable sites identified in Tables 3 and 4, was calculated (Table 5). Defect energies are defined with respect to the perfect lattice and the substituted ions at infinity. It can be seen that the difference in the substitutional defect energy of the V^{3+} ion at the most and least stable aluminium sites is significant, confirming the previous result that T,Al(5) would be preferably occupied by the V^{3+} ion if substitution is *via* this mechanism. In the substitution of P^{5+} by V^{5+} the same defect energy was obtained for all six non-equivalent sites, again corroborating the perfect lattice calculations.

An energetic comparison between the two cases of Al^{3+} or P^{5+} substitution (VAPO† and VAPO††) is not possible because the absolute defect energies calculated are valid only for different configurations of a particular structure, not for different oxidation states. However, we are able to investigate the changes in the local geometry (T–O distances and angles) resulting from the substitution of the vanadium. These changes will make a significant contribution to the defect energy. The

Table 2 Energy, unit cell parameters and volume of the unit cell from the optimization of VAPO-5 (the starting point was the hexagonal *P6cc* unit cell of Bennett)[14]

Cell	E^a /eV	*a*/Å	*b*/Å	*c*/Å	α/°	β/°	γ/°	*V*/Å^3
Experimental[34]	—	13.71	13.71	8.46	90.00	90.00	120.00	1375
VAPO†^{b}	−267.0938	13.83	14.01	8.47	89.63	90.13	120.47	1413
VAPO††^{c}	−266.8993	13.83	13.86	8.45	89.99	89.88	120.32	1398

^{a}Energy per TO_4 unit of $AlPO_4$-5, T = Al, P. $^b V^{3+}$ in aluminium sites of a hexagonal *P6cc* unit cell. $^c V^{5+}$ in phosphorus sites of a hexagonal *P6cc* unit cell.

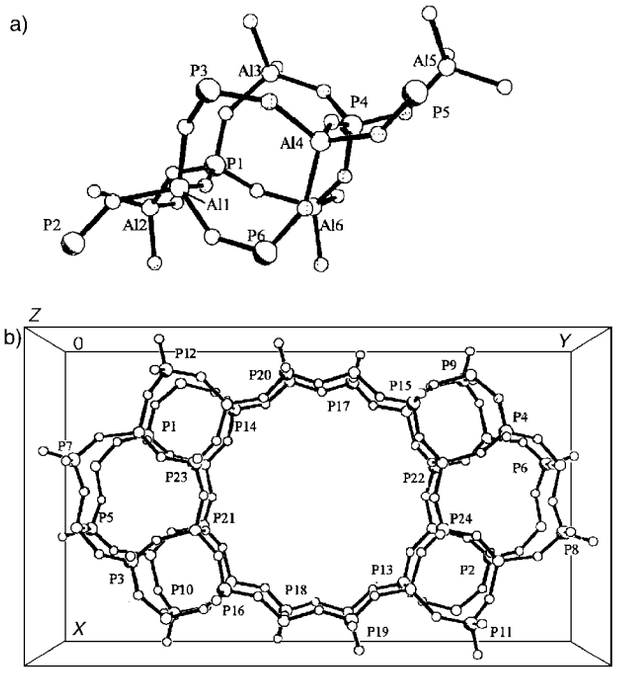

Fig. 1 Orthorhombic *Pcc*2 unit cell of $AlPO_4$-5 viewed along the *c*-axis. a) asymmetric unit cell b) tetrahedral phosphorus sites in the $AlPO_4$-5 unit cell.

other contribution is the long-range perturbation of the electrostatic potential of the material due to the substitution. This problem has been discussed extensively by Sastre and Lewis in a recent paper.[36]

The T–O distances and O–T–O, T–O–P angles for the twelve configurations of interest are shown in Table 6. The V^{3+}–O distances are approximately 0.3 Å larger than the corresponding Al^{3+}–O distance in $AlPO_4$-5. The least stable configuration T,Al(3) has the lowest distance V^{3+}–O. The angles V^{3+}–O–P in the T,Al(3) vary significantly (139.3°–171.1°) with respect to those in the parent $AlPO_4$-5 structure (144.8°–155.3°), indicating a very strong deformation of the framework in the proximity of the substituted site. However, an analysis of the O–V^{3+}–O angles does suggest a general correlation between O–T–O deformation and stability. Nevertheless, an important distortion of the site is observed due to the introduction of the defect. The strong local distortion produced by V^{3+} incorporation in aluminium sites may therefore lead to an unstable structure of VAPO-5 and finally to the collapse of the structure. That is to say, the lattice only permits substitutions which cause small changes in the geometry. We therefore, suggest that the substitution of Al^{3+} by V^{3+} is unfavourable in the $AlPO_4$-5 framework. Indeed, we note that in a temperature programmed reduction (TPR) study[8] of VAPO-5 the $V^{4+} \rightarrow V^{3+}$ redox process is possible only with a collapse of the framework structure.

The incorporation of V^{5+} in the phosphorus site leads to a significantly smaller deformation of the tetrahedral sites. The V^{5+}–O distances are approximately 0.1 Å longer than the P^{5+}–O distances in $AlPO_4$-5. The V^{5+}–O–Al angles are only five degrees larger than the Al–O–P angles in $AlPO_4$-5. It can be seen that these distortions are much smaller than those found for the substitution of Al^{3+} by V^{3+}. Concerning the O–T–O angles we obtain a smaller change in minimum and maximum angles (107.20°–111.20°) than for the substitution of Al^{3+} by V^{3+}. Thus, our results would suggest that upon calcination vanadium, as V^{5+}, is likely to be found substituted at phosphorus sites in the $AlPO_4$-5 framework, in agreement with previous results.[4,5,8,12,13]

Moreover, we have investigated the behaviour of the long-range interactions in $AlPO_4$-5 and VAPO-5. In the $AlPO_4$-5 structure a similar electrostatic potential for the 24 tetrahedral phosphorus sites is obtained (see Figs. 1b and 2). This result helps us to understand the similarities between the different phosphorus sites in their substitution by V^{5+}. In the VAPO-5, the presence of the V^{5+} in the tetrahedral phosphorus sites produces a significant "perturbation" of the electrostatic potential with respect to pure $AlPO_4$-5. The difference between the electrostatic potential in the vanadium and the phosphorus sites ($\approx$6.0 V) may be a factor in explaining the activity of vanadium sites for catalytic processes.

3.2 Substitution of two P^{5+} ions by V^{5+} ions in tetrahedral sites

In order to study the dependence of the geometry of the unit cell on the amount of vanadium incorporated in the framework and possible interactions between V^{5+} sites, we carried out a simulation of the 78 non-equivalent configurations corresponding to two ions of V^{5+} in tetrahedral phosphorus sites per $AlPO_4$-5 unit cell. The energies of the four most and least stable configurations are shown in Table 7. The labels of each position are similar to those shown in Fig. 1b (in this case we work with 24 tetrahedral sites). We did not find any relationship between the stability of the framework and the position of

Table 3 Energies and parameters of the cell for the substitution of Al^{3+} by V^{3+} in the six different independent sites of the orthorhombic *Pcc*2 unit cell of Mora *et al.*[23]

Site	*E*/eV^a	*a*/Å	*b*/Å	*c*/Å	α/°	β/°	γ/°	*V*/Å^3
T,Al(1)	−267.5789	13.795	24.025	8.439	89.90	89.94	90.46	2796.74
T,Al(2)	−267.5789	13.814	23.973	8.447	90.05	90.15	89.57	2797.31
T,Al(3)	−267.5733	13.880	23.841	8.448	90.00	90.03	90.17	2795.42
T,Al(4)	−267.5771	13.816	23.982	8.454	89.80	89.94	89.94	2801.12
T,Al(5)	−267.5797	13.804	23.992	8.441	90.03	89.99	89.99	2795.67
T,Al(6)	−267.5780	13.864	23.856	8.443	90.12	89.91	89.91	2792.36

^{a}Energy per AlO_4 unit of $AlPO_4$-5.

Table 4 Energies and parameters of the cell for the substitution P^{5+} by V^{5+} in the six different independent sites of the orthorhombic *Pcc*2 unit cell of Mora *et al.*[23]

Site	*E*/eV[a]	*a*/Å	*b*/Å	*c*/Å	*α*/°	*β*/°	*γ*/°	*V*/Å^3
T,P(1)	−267.4829	13.779	23.891	8.412	90.02	89.99	90.19	2769.20
T,P(2)	−267.4829	13.770	23.906	8.412	89.98	89.99	89.84	2769.09
T,P(3)	−267.4824	13.811	23.838	8.413	90.02	90.02	89.95	2769.64
T,P(4)	−267.4829	13.779	23.891	8.412	89.99	89.99	90.19	2769.33
T,P(5)	−267.4829	13.770	23.906	8.412	89.99	89.99	89.84	2769.11
T,P(6)	−267.4824	13.811	23.838	8.413	90.02	90.02	89.95	2769.61

[a]Energy per PO_4 unit of $AlPO_4$-5.

Table 5 Calculated isolated defect energies corresponding to the two most and least stable structures of Tables 3 and 4

Substitution	Site	*E*/eV[a]	E_{defect}/eV
	T,Al(5)	−267.5797	7.999
Al^{3+} by V^{3+}	T,Al(3)	−267.5733	8.138
	T,P(2)	−267.4829	12.464
P^{5+} by V^{5+}	T,P(3)	−267.4824	12.484

[a]Energy per PO_4 unit of $AlPO_4$-5.

the vanadium ions substituted. This could be a consequence of the fact that only small geometric changes occur on the introduction of the V^{5+} ion into the framework. An increase of about 1% in the unit cell volume was found for configurations where one V^{5+} per unit cell was obtained. An increase in cell volume with the quantity of vanadium has been reported by Blasco *et al.*[8] for samples with a vanadium content similar to our simulation ($\approx$1.2 vanadium atom per unit cell in uncalcined VAPO-5).

The changes in the *a* and *c* unit cell parameters with the vanadium content are shown in Figs. 3 and 4. A similar trend for both parameters was reported experimentally by Blasco *et al.*[8] In particular, we found that the *c* parameter decreases when the V^{5+} content varies between 0 and 1.2 V^{5+} ions per unit cell as in the experiment. For a V^{5+} content higher than 1.2 ions per unit cell the simulated *c* parameter increases. It has been reported experimentally that VAPO-5 with a vanadium content higher than 3 wt% (corresponding to 1.2 vanadium atoms per unit cell) shows a low crystallinity. Probably, the anomalous behaviour of the simulated *c* parameter for the case of two V^{5+} is related to this fact. Jhung *et al.*[5] have reported changes of *a* and *c* parameters of the order of 0.01–0.02 Å for samples with a low vanadium content.

In Fig. 5 the dependence of the volume of the unit cell on the total energy of the cell for the four most and least stable configurations is shown. The four least stable configurations have a cell volume about 0.5% higher than the four most stable. This result could be interpreted as a consequence of the deformations of the cell in the least stable configurations due to the presence of the V^{5+} ion.

3.3 Simulation of the vibrational spectrum for $AlPO_4$-5 and VAPO-5

In Fig. 6 we show the vibrational spectrum derived by lattice dynamical calculations using the above described potentials and the experimental IR[19] spectrum of $AlPO_4$-5. The fundamental frequencies are in good agreement with the experi-

Table 6 Bond distances and O–T–O, T–O–P angles for the substitution of Al^{3+} by V^{3+} and P^{5+} by V^{5+}

$AlPO_4$-5[a]				Substitution of Al^{3+} by V^{3+}			
Site	Al–O/Å	O–Al–O/°	Al–O–P/°	Site	V–O/Å	O–V^{3+}–O/°	V–O–P/°
Al(1)	1.710–1.727	106.73–112.65	144.93–156.52	T,Al(1)	2.010–2.036	100.56–114.28	143.72–158.04
Al(2)	1.710–1.732	104.32–112.81	140.14–156.44	T,Al(2)	2.010–2.050	97.94–113.94	147.23–155.57
Al(3)	1.712–1.728	105.07–112.89	144.82–155.32	T,Al(3)	2.001–2.074	110.30–115.09	139.27–171.06
Al(4)	1.710–1.727	106.72–112.66	144.94–156.16	T,Al(4)	2.008–2.040	100.18–114.19	146.47–156.68
Al(5)	1.710–1.732	104.32–112.81	140.13–156.43	T,Al(5)	2.004–2.027	98.49–114.36	147.57–156.94
Al(6)	1.712–1.728	105.07–112.90	144.82–155.32	T,Al(6)	2.014–2.044	99.11–113.93	141.66–156.85
$AlPO_4$-5[a]				Substitution of P^{5+} by V^{5+}			
Site	V–O/Å	O–P–O/°	P–O–Al/°	Site	V–O/Å	O–V^{5+}–O/°	V–O–Al/°
P(1)	1.507–1.529	107.99–110.50	142.91–156.52	T,P(1)	1.601–1.624	107.23–111.15	148.94–160.46
P(2)	1.508–1.530	108.16–110.42	144.15–156.44	T,P(2)	1.601–1.624	107.21–111.17	148.82–160.31
P(3)	1.504–1.528	108.47–109.95	142.04–155.32	T,P(3)	1.600–1.624	107.45–110.79	148.82–160.33
P(4)	1.506–1.529	107.98–110.52	142.94–156.52	T,P(4)	1.601–1.624	107.23–111.15	148.96–160.50
P(5)	1.509–1.530	108.15–110.42	144.15–156.43	T,P(5)	1.600–1.624	107.20–111.17	148.82–160.32
P(6)	1.504–1.528	108.46–109.95	142.04–155.32	T,P(6)	1.600–1.624	107.44–110.79	148.82–160.31

[a]$AlPO_4$-5 optimised.

Table 7 Energies and unit cell parameters of the four most and least stable configurations of two V^{5+} in the $AlPO_4$-5 unit cell

T-site[a]	*E*/eV[b]	*a*/Å	*b*/Å	*c*/Å	*α*/°	*β*/°	*γ*/°	*V*/Å^3
1 2	**−266.9022**	**13.798**	**23.949**	**8.430**	**90.00**	**90.00**	**90.37**	**2785.78**
13 14	**−266.9022**	**13.798**	**23.949**	**8.446**	**90.00**	**90.00**	**90.37**	**2785.79**
5 16	**−266.9015**	**13.793**	**23.972**	**8.436**	**89.99**	**89.97**	**89.76**	**2789.26**
13 21	**−266.9013**	**13.827**	**23.918**	**8.431**	**89.98**	**90.13**	**90.14**	**2788.12**
1 3	−266.8971	13.814	23.974	8.457	90.02	90.20	90.20	2800.52
21 23	−266.8969	13.848	23.904	8.449	90.00	90.10	90.10	2796.81
5 19	−266.8968	13.778	24.058	8.458	90.96	90.00	90.00	2803.60
9 22	−266.8967	13.831	23.937	8.453	90.00	89.53	89.53	2798.48

[a]The most stable configurations are shown in bold. [b]Energy per PO_4 unit of $AlPO_4$-5.

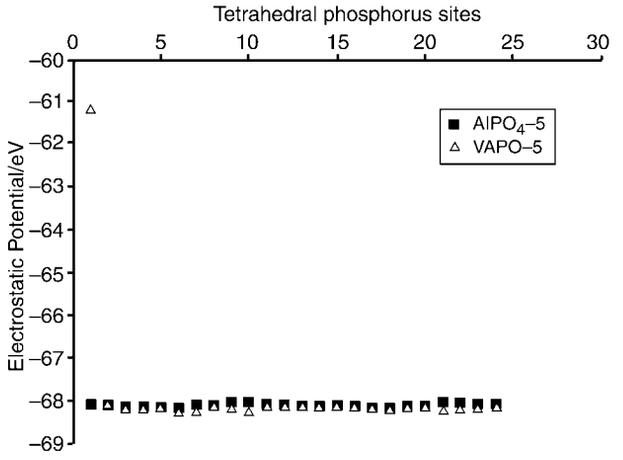

Fig. 2 Electrostatic potential in the phosphorus sites (simulated), square: $AlPO_4$-5, triangle: VAPO-5 with V^{5+} in the T(1) site of the $AlPO_4$-5 unit cell.

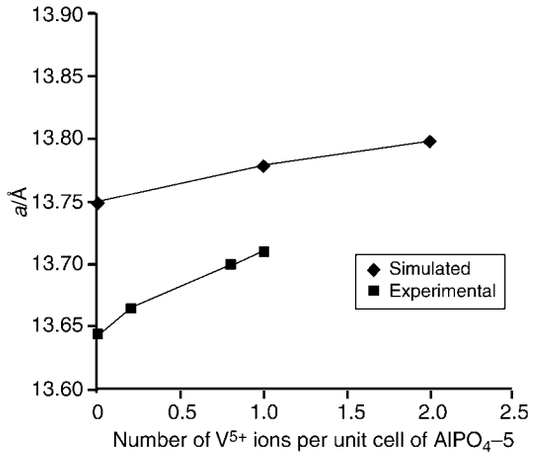

Fig. 3 Dependence of the *a* parameter on the amount of V^{5+} ion in the VAPO-5 unit cell.

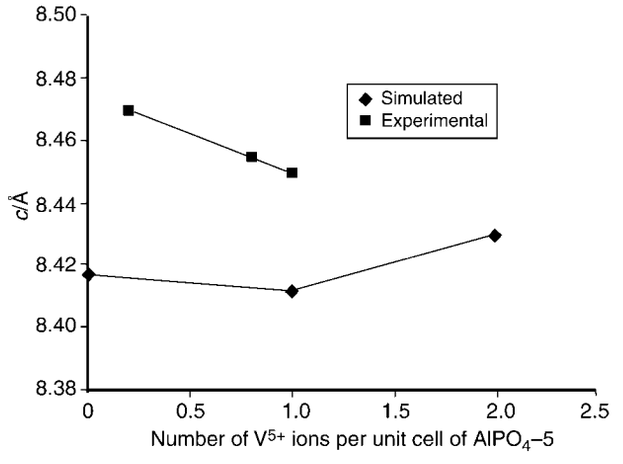

Fig. 4 Dependence of the *c* parameter on the amount of V^{5+} ion in the VAPO-5 unit cell.

mental data. The band at 1000–1200 cm^{-1} attributed to asymmetric stretching of tetrahedral PO_4 is well reproduced. Similarly, we find the band at 712 cm^{-1} attributed to symmetric stretching of P–O and the bands at 459 cm^{-1} (P–O bending) and between 500–650 cm^{-1} (vibrations in the double ring region). The simulated intensities are not well reproduced due to the classical model used.

Fig. 7 shows the simulated VAPO-5 vibrational spectra for a

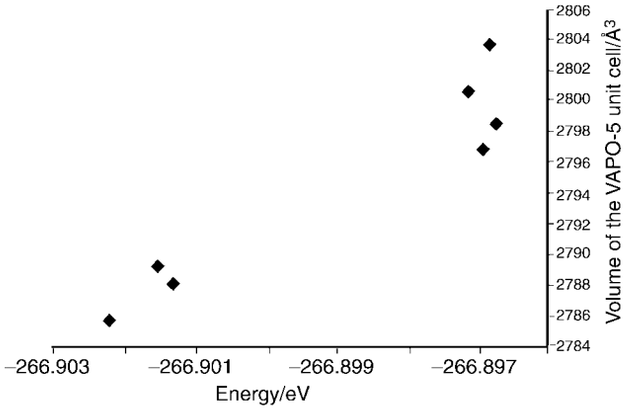

Fig. 5 Dependence of the cell volume on the total energy of the unit cell for the eight most and least stable configurations for two V^{5+} ions substituted into the $AlPO_4$-5 unit cell.

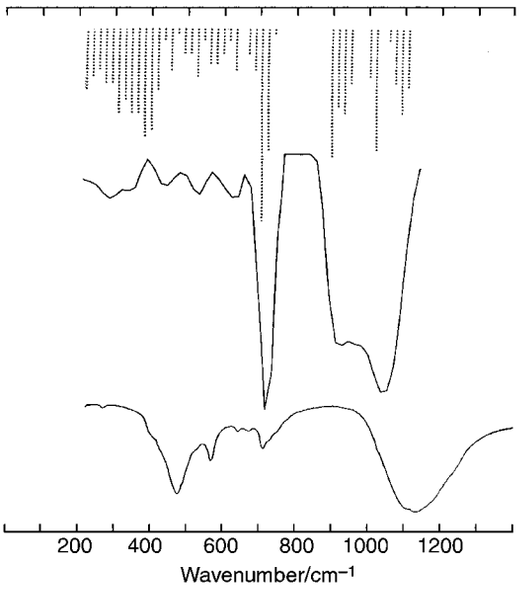

Fig. 6 Simulated vibrational spectrum and IR spectrum[19] of the $AlPO_4$-5. Up: calculated, down: experimental

structure with V^{3+} ions (Fig. 7a) and V^{5+} ions (Fig. 7b) in the unit cell. These spectra are very similar to the IR spectrum of $AlPO_4$-5, the main difference being a new band at ≈830–840 cm^{-1} in the last spectrum (see Fig. 7b). The intensity of this band increases with the amount of V^{5+} ion in the unit cell. The band at 835 cm^{-1} has previously been assigned to isolated tetrahedral V^{5+} species,[9] an assignment supported here.

Analysis of eigenvalues of the dynamical matrix and their corresponding vibrational frequencies confirm the above result. The calculated phonon spectrum of VAPO-5 shows only real vibrational modes, indicating that a true minimum was obtained. On the other hand, the simulated vibrational spectrum of the VAPO-5 with V^{3+} in aluminium sites does not show the additional band at ≈835 cm^{-1} (Fig. 7a). Thus, we think that the presence of this new band in VAPO-5 with V^{5+} in phosphorus sites is very strong evidence of the incorporation in tetrahedral phosphorus sites.

Conclusions

The most important conclusion of this paper is that the substitution of Al^{3+} by V^{3+} in the tetrahedral sites of the $AlPO_4$-5 framework leads to a great disorder in the structure, while the incorporation of V^{5+} in phosphorus sites leads to comparatively smaller deformations of the framework. The

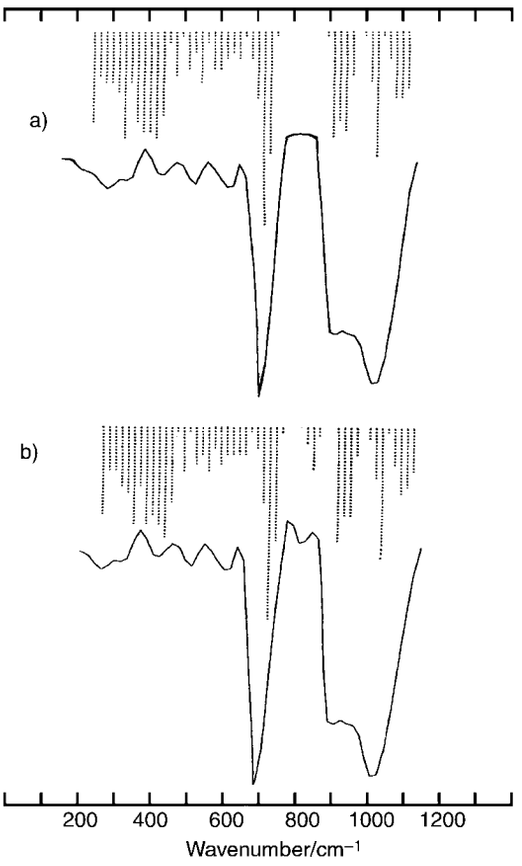

Fig. 7 Simulated vibrational spectrum of VAPO-5. a) With one V^{3+} per unit cell of $AlPO_4$-5; b) With two V^{5+} per unit cell of $AlPO_4$-5. The new band near to 835 cm^{-1} is shown.

V^{3+}–O distances are incremented $\approx$0.3 Å with respect to Al^{3+}–O distances in $AlPO_4$-5. The V^{3+}–O–P and O–V^{3+}–O angles present a great variation with respect to $AlPO_4$-5. In contrast, for substitution of P^{5+} by V^{5+} the changes of the V^{5+}–O, V^{5+}–O–Al and O–V^{5+}–O with respect to $AlPO_4$-5 are much smaller. Therefore, we consider the likely substitution mechanism to be that of P^{5+} by V^{5+}. For this substitution our calculations indicate that the V^{5+} ion can occupy any of the six phosphorus sites in the orthorhombic unit cell.

For the case of two V^{5+} ions in the phosphorus sites we did not find a relationship between the stability of the framework and the position of the vanadium ions substituted. An increment of 1% in the volume of the unit cell with respect to the configurations of one V^{5+} ions was obtained. The simulation of the IR spectrum shows a new band (not found in $AlPO_4$-5) associated with an isolated tetrahedral V^{5+} species corresponding to the experimental result. In future work we will undertake the study of the substitution of vanadium with other valence states (V^{4+}) in the $AlPO_4$-5 framework.

Acknowledgements

We are grateful to Professor G. B. Suffritti (University di Sassari) and Dr A. R. Ruiz-Salvador(University de La Habana) for comments and critical reading.

References

1 E. M. Flaningen, B. M. Lok, R. L. Patton and S. T. Wilson, *Proc. Int. Zeolite Conf. 7th*, 1986, 103.
2 G. Bellussi and M. S. Rigutto, in *Advanced Zeolite Science and Applications*, J. C. Jansen, M. Stocker, H. G. Karge and J. Weitkamp eds., Elsevier, Amsterdam, 1994, p. 177.
3 M. S. Rigutto and H. J. van Bekkum, *J. Mol. Catal. A*, 1993, **81**, 77.
4 C. Montes, M. E. Davis, B. Murray and M. Naryana, *J. Phys. Chem.*, 1990, **94**, 6425.
5 S. H. Jhung, Y. S. Uh and H. Chon, *Appl. Catal.*, 1990, **62**, 61.
6 A. Miyamoto, Y. Iwamoto, Y. Matsuda and T. Inui, *Stud. Surf. Sci. Catal.*, 1990, **49B**, 1233.
7 P. Concepción, J. M. López Nieto and J. Pérez-Pariente, *Catal. Lett.*, 1993, **13**, 333.
8 T. Blasco, P. Concepción, J. M. López Nieto and J. Pérez-Pariente, *J. Catal.*, 1995, **152**, 1.
9 P. Concepción, J. M. López Nieto and J. Pérez-Pariente, *J. Mol. Catal. A.*, 1995, **99**, 173.
10 B. M. Weckhuysen, I. P. Vannijvel and R. A. Schoonheydt, *Zeolites*, 1995, **15**, 482.
11 A. Martin, H. Berndt, U. Lohse and B. Lücke, *React. Kinet. Catal. Lett.*, 1995, **56**, 37.
12 F. Bedioui, E. Briot, J. Devynck and K. J. Balkus, *Inorg. Chim. Acta*, 1997, **254**, 151.
13 A. M. Prakash and L. Kevan, *J. Phys. Chem.*, 1999, **103**, 2214.
14 J. Bennett, J. P. Cohen, E. M. Flanigen, J. J. Pluth and J. V. Smith, in *Intrazeolite Chemistry*, G. D. Stucky and F. G. Dwyer eds., ACS Symposium Series 218, American Chemical Society, Washington DC, 1983, p 109.
15 S. Qiu, Q. Pang, H. Kessler and J. L. Guth, *Zeolites*, 1989, **8**, 440.
16 J. W. Richardson, J. Pluth and J. V. Smith, *Acta Crystallogr., Sect. C.*, 1987, **43**, 1469.
17 M. P. Peeters, L. van de Ven, J. W. de Haan and J. H. van Hooff, *J. Phys. Chem.*, 1995, **97**, 9254.
18 E. de H. vos Burchart, H. J. van Bekkum, B. van de Graaf and E. T. C. Vogt, *J. Chem. Soc., Faraday Trans.*, 1992, **88**, 2761.
19 A. J. M. de Man, W. P. J. H. Jacobs, J. P. W. Gilson and R. A. van Santen, *Zeolites*, 1992, **12**, 826.
20 G. Sastre, D. W. Lewis and C. R. A. Catlow, *J. Phys. Chem.*, 1996, **100**, 6722.
21 G. Sastre, D. W. Lewis and C. R. A. Catlow, *J. Phys. Chem. B*, 1997, **101**, 5249.
22 N. J. Henson, A. K. Cheetham and J. D. Gale, *Chem. Mater.*, 1996, **8**, 664.
23 A. J. Mora, A. N. Fitch, M. Cole, R. Goyal, R. H. Jones, H. Jobic and S. W. Carr, *J. Mater. Chem.*, 1996, **6**, 1831.
24 A. R. Ruiz-Salvador, G. Sastre, D. W. Lewis and C. R. A. Catlow, *J. Mater. Chem.*, 1996, **6**, 1837.
25 J. D. Gale, *J. Chem. Soc., Faraday Trans.*, 1997, **93**, 629.
26 P. P. Ewald, *Ann. Physik*, 1921, **64**, 253.
27 B. G. Dick and A. W. Overhauser, *Phys. Rev.*, 1958, **112**, 90.
28 D. F. Shanno, *Math. Comp.*, 1970, **24**, 647.
29 J. Simons, P. Jørgensen, H. Taylor and J. Ozment, *J. Phys. Chem.*, 1983, **87**, 2745.
30 N. F. Mott and M. J. Littleton, *Trans. Faraday Soc.*, 1938, **38**, 485.
31 J. D. Gale and N. J. Henson, *J. Chem. Soc., Faraday Trans.*, 1994, **90**, 3175.
32 D. C. Sayle, C. R. A. Catlow, M. A. Perrin and P. Nortier, *J. Phys. Chem. Solids*, 1995, **56**, 799.
33 J. Gulín-González, J. de la Cruz Alcaz, A. R. Ruiz-Salvador, A. Gómez, A. Dago and C. de las Pozas, *Micropor. Mesopor. Mater.*, 1999, **29**, 361.
34 P. Concepción, J. M. López Nieto, A. Mifsud and J. Pérez-Pariente, *App. Catal. A*, 1997, **151**, 373.
35 N. Tielen, M. Geelen and P. A. Jacobs, *Acta Phys. Chem.*, 1985, **31**, 1.
36 G. Sastre and D. W. Lewis, *J. Chem. Soc., Faraday Trans.*, 1998, **94**, 3049.